Experimental determination of electron states with orbital degrees of freedom

The orbital degree of freedom plays an important role in strongly correlated materials. Several direct observation methods of electron orbitals have been proposed, but they usually focus on the orbital ordered or stable state, and there are few reports on the observation of the degenerate orbitals. Even first-principles calculations cannot easily determine metastable states at finite temperatures. Therefore, the electron state in degenerate orbitals is only vaguely understood.

Recently, our group has proposed the core differential Fourier synthesis (CDFS) method [1]. It allows the direct observation of the 3D distribution of the valence electron density (VED) by synchrotron X-ray diffraction (XRD). It has been successfully applied to determine the electron density in the orbital ordered state and reported in the Research Frontiers 2020. In the work discussed here [2], we used it to determine the electron state with orbital degrees of freedom through the VED distribution.

We investigated the orbital state of vanadium spinel oxide FeV_2O_4. In this system, despite the lack of charge degrees of freedom due to the Mott insulator, both electronic correlations and geometric frustration are present, resulting in an interplay between the different degrees of freedom, such as spin, orbital, and lattice, which leads to three successive phase transitions with decreasing temperature [3]. Although there has been much discussion on the origin of the phase transition, mainly focusing on the orbital ordered state of V, there are few reports of the definitive determination of the electronic state of the high-symmetry cubic phase.

In FeV_2O_4, because the formal charges of Fe and V are +2 and +3, the electron configurations are $3d^6$ and $3d^2$, respectively. The space group of the cubic phase is $Fd\bar{3}m$, and because FeO_4 is a regular tetrahedron, the electron configuration of Fe^{2+} is $e^3t_2^3$. Owing to the high-spin configuration, one electron on the e orbital is responsible for the orbital degree of freedom (Fig. 1(b)). By contrast, the octahedral site of VO_6 has inversion symmetry, and the $3d$ orbitals of V^{3+} are divided into lower triply degenerate t_{2g} orbitals and higher doubly degenerate e_g orbitals. If VO_6 forms a regular octahedron (O_h), then $3d^2$ electrons occupy t_{2g} in a high-spin configuration (Fig. 1(b)), and V^{3+} has spin and orbital degrees of freedom. Therefore, the FeV_2O_4 system in the cubic phase has spin and orbital degrees of freedom at both the Fe^{2+} and V^{3+} sites. However, the $3d$ state is complicated because of a slight D_{3d} distortion in the VO_6 octahedron.

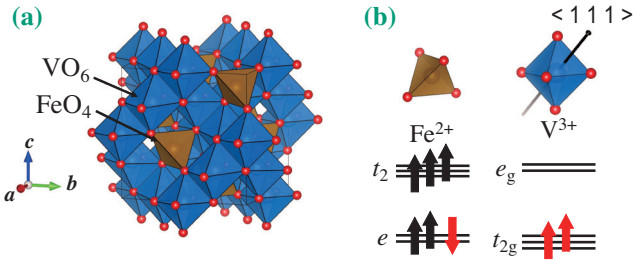

Fig. 1. **(a)** Crystal structure of FeV_2O_4 in the cubic phase. **(b)** Orbital states of V and Fe in the cubic phase. The black arrow in VO_6 indicates the <1 1 1> direction.

The triply degenerate t_{2g} orbitals are further split into one orbital (φ_1) and degenerate orbitals (φ_2 and φ_3) by the crystal field formed by the surrounding oxygen. However, it is not clear which energy level is higher, φ_1 or degenerate orbitals. It is important to note that the triple degeneracy of the t_{2g} orbitals is maintained when the effect of the D_{3d}-type strain is very weak compared with that of the thermal fluctuation. Therefore, we attempted to determine the correct orbital state from the 3D distribution of VED obtained by the CDFS method.

XRD experiments were performed using single crystals at SPring-8 **BL02B1**. Figure 2(d) shows the observed VED around the V (1/2 1/2 1/2) site at 160 K. The VED around the V site is clearly anisotropic. This VED directly reflects the anisotropy of the $3d^2$ electrons.

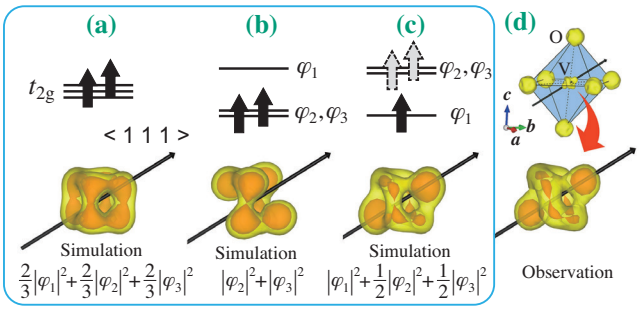

Fig. 2. **(a–c)** Assumed electron configurations and simulated VEDs of V site. The red part of the VED highlights the characteristic components. The gray dotted arrows in (c) indicate that one electron on double degenerate orbitals occupies both orbitals with equal probability. **(d)** (upper panel) Observed VED of VO6 octahedron with internal coordinates (1/2 1/2 1/2) (isosurface level $4.5e/Å^3$). The solid line indicates the octahedron and the dotted line indicates the V–O bonds. (lower panel) Observed VED at V site (isosurface level $4.5e/Å^3$ (yellow) and $5.3e/Å^3$ (orange)).

First, we assumed three orbital states as mentioned above, but the VEDs simulated simply from these states did not reproduce the observed one well (Figs. 2(a,b)). However, we found another possible orbital state where φ_1 was stabilized. In general, the energy gap of the t_{2g} orbitals due to the D_{3d} distortion is small, and Hund's rules are considered. In this case, one electron occupied the lower φ_1 and the other one was lifted to the degenerate orbitals. The simulation $|\varphi_1|^2 + \frac{1}{2}|\varphi_2|^2 + \frac{1}{2}|\varphi_3|^2$ resulted in the VED distribution shown in Fig. 2(c), which perfectly reproduced the experimental result. It is noted that we also succeeded in determining the orbital state at the Fe site. VED analysis by the CDFS method revealed that the degenerate orbitals reflect the anisotropy of their constituent orbitals in the cubic phase.

Here, we reconsider the degenerate orbital. We find that the wavefunctions can also be represented with an arbitrary value of phase θ as

$$\begin{cases} \varphi_2'(\boldsymbol{r}) = \varphi_2(\boldsymbol{r})\cos\theta(\boldsymbol{r},t) + \varphi_3(\boldsymbol{r})\sin\theta(\boldsymbol{r},t) \\ \varphi_3'(\boldsymbol{r}) = -\varphi_2(\boldsymbol{r})\sin\theta(\boldsymbol{r},t) + \varphi_3(\boldsymbol{r})\cos\theta(\boldsymbol{r},t) \end{cases}$$

Orbital degrees of freedom mean that θ fluctuates in space and time. However, from the diffraction data, it is not clear that θ fluctuates in space and time because the VED obtained by XRD measurements is both space- and time-averaged. In fact, assuming an orbital glass state with θ distributed in the whole crystal only spatially, the experimental results can also be reproduced from the θ spatial average.

$$\frac{1}{2\pi}\int_0^{2\pi}(|\varphi_1|^2 + |\varphi_2\cos\theta + \varphi_3\sin\theta|^2)\,d\theta = |\varphi_1|^2 + \frac{1}{2}|\varphi_2|^2 + \frac{1}{2}|\varphi_3|^2$$

Therefore, we investigated the dynamics of FeV_2O_4 through phonons to confirm that θ fluctuates in space and time. If θ fluctuates in time, we expect that electron-phonon coupling will allow the electron orbital fluctuations to affect the phonon behavior. In particular, phonon softening might be observed toward the phase transition where orbital fluctuations are eliminated. Therefore, we performed inelastic X-ray scattering (IXS) at SPring-8 **BL43LXU**. The softening of the transverse acoustic (TA) mode dispersing along the [1 1 0] and polarized along [–1 1 0] was clearly observed, as shown in Fig. 3. The symmetry of this TA mode is E_g, which means θ fluctuations. Also, as shown in the dispersion diagram of the E_g TA mode in Fig. 3(c), the softening of the E_g TA mode was observed up to $q \sim 0.7$ r.l.u. This softening is different from the usual precursor phenomenon of structural phase transitions but resembles the nematic state of iron-based superconductors, in which orbital degrees of freedom play an important role [4].

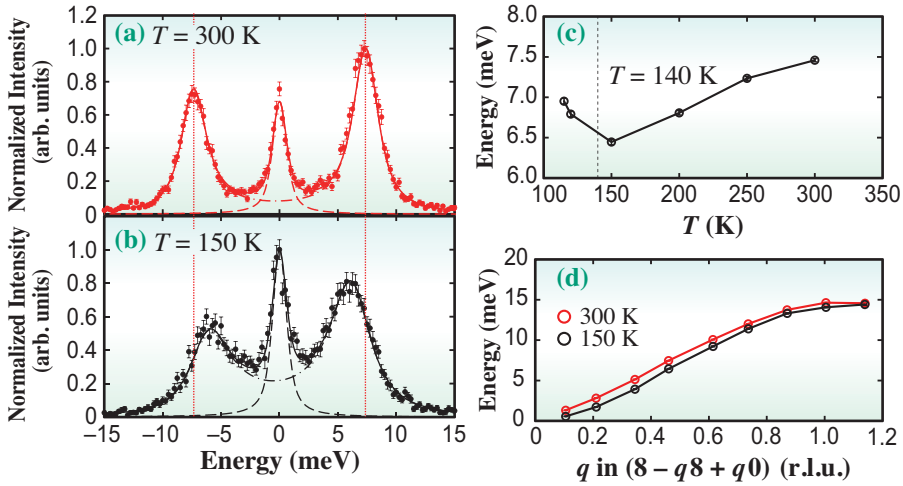

Fig. 3. Energy scan data at Q = (7.54 8.45 –0.03) at **(a)** 300 K and **(b)** 150 K. Phonon peaks correspond to the E_g TA mode. Solid lines indicate the results of fitting using two lines, corresponding to an elastic peak (dashed line) and a pair of phonon peaks (dash-dotted line). The vertical dotted line indicates the phonon energy at 300 K. **(c)** Temperature dependence of the phonon energy at Q = (7.54 8.45 –0.03). **(d)** Phonon dispersions of the E_g TA mode at 300 K and 150 K.

Taishun Manjo[a,*] and Hiroshi Sawa[b]

[a] Japan Synchrotron Radiation Research Institute (JASRI)
[b] Department of Applied Physics, Nagoya University

*Email: manjo.taishun@spring8.or.jp

References

[1] S. Kitou *et al.*: Phys. Rev. Res. **2** (2020) 033503.
[2] *T. Manjo, S. Kitou, N. Katayama, S. Nakamura, T. Katsufuji, Y. Nii, T. Arima, J. Nasu, T. Hasegawa, K. Sugimoto, D. Ishikawa, A. Q. R. Baron and H. Sawa: Mater. Adv. **3** (2022) 3192.*
[3] Y. Nii *et al.*: Phys. Rev. B **86** (2012) 125142.
[4] A.M. Merritt *et al.*: Phys. Rev. Lett. **124** (2020) 157001.